Phospholemman Deficiency in Postinfarct Hearts: Enhanced Contractility but Increased Mortality

M. Ayoub Mirza, M.D.[1,2], Susan Lane, M.D.[1,2], Zequan Yang, Ph.D.[2], Themis Karaoli, Ph.D.[2], Kwame Akosah, M.D.[1], John Hossack, Ph.D.[3], Marcia McDuffie, M.D.[4], JuFang Wang, M.D.[5], Xue-Qian Zhang, M.D.[5], Jianliang Song, M.D., Ph.D.[5], Joseph Y. Cheung, M.D., Ph.D.[5], and Amy L. Tucker, M.D.[1,2,6]

Abstract

Phospholemman (PLM) regulates $[Na^+]_i$, $[Ca^{2+}]_i$ and contractility through its interactions with Na^+-K^+-ATPase (NKA) and Na^+/Ca^{2+} exchanger (NCX1) in the heart. Both expression and phosphorylation of PLM are altered after myocardial infarction (MI) and heart failure. We tested the hypothesis that absence of PLM regulation of NKA and NCX1 in PLM-knockout (KO) mice is detrimental. Three weeks after MI, wild-type (WT) and PLM-KO hearts were similarly hypertrophied. PLM expression was lower but fractional phosphorylation was higher in WT-MI compared to WT-sham hearts. Left ventricular ejection fraction was severely depressed in WT-MI but significantly less depressed in PLM-KO-MI hearts despite similar infarct sizes. Compared with WT-sham myocytes, the abnormal $[Ca^{2+}]_i$ transient and contraction amplitudes observed in WT-MI myocytes were ameliorated by genetic absence of PLM. In addition, NCX1 current was depressed in WT-MI but not in PLM-KO-MI myocytes. Despite improved myocardial and myocyte performance, PLM-KO mice demonstrated reduced survival after MI. Our findings indicate that alterations in PLM expression and phosphorylation are important adaptations post-MI, and that complete absence of PLM regulation of NKA and NCX1 is detrimental in post-MI animals. Clin Trans Sci 2012; Volume 5: 235–242

Keywords: FXYD proteins, sudden death, excitation-contraction coupling

Introduction

Phospholemman (PLM) is the product of a single copy gene encoding a 15-kDa sarcolemmal protein abundantly expressed in heart.[1] PLM belongs to a family of small (30- to 130- amino acid) single membrane-spanning proteins involved in ion transport regulation. In 2000, Sweadner and Rael named this family "FXYD," after a conserved signature sequence in the N-terminus.[2] As a family, FXYD members are found predominantly in tissues that are involved in solute and fluid transport (kidney, colon, mammary gland, pancreas, prostate, liver, lung, and placenta) or that are electrically excitable (heart, skeletal muscle, and nervous system). This is consistent with their function as regulators of ion transporters and/or channel activity.[3–7] At least 5 of 10 known FXYD proteins including PLM modulate the function of Na^+-K^+-ATPase (NKA), each with distinct effects, allowing for tissue- and site-specific regulation. In mammalian cardiac myocytes, PLM regulates the activities of both NKA and the cardiac Na^+/Ca^{2+} exchanger (NCX1).[8–13]

PLM possesses multiple phosphorylation sites, including consensus sites for protein kinases (PKs) A and C, myotonic dystrophy kinase, and never-in-mitosis A kinase.[14–16] In the heart, PLM is the major sarcolemmal substrate for PKA and PKC.[1,17] PLM is phosphorylated at Ser68 by PKA and at both Ser68 and Ser63 by PKC.[15] Phosphorylation of PLM by PKA or PKC relieves its inhibition of NKA by increasing Na^+ affinity[18–20] or V_{max},[9,19–21] while simultaneously inhibiting NCX1.[22] Isoproterenol has no effect on NKA activity in PLM-knockout (KO) cardiac myocytes.[18,20]

In response to pacing (2 Hz) and β-adrenergic stimulation, PLM-KO cardiac myocytes exhibit monotonic increases in $[Na^+]_i$ whereas wild-type (WT) myocytes show a time-dependent decline in $[Na^+]_i$.[20] This is due to enhancement of NKA activity in WT but not PLM-KO myocytes. In addition, on cessation of pacing, PLM-KO myocytes treated with β-adrenergic agonists have increased spontaneous $[Ca^{2+}]_i$ transients and contractions.[23] *In vivo*, in response to isoproterenol stimulation, $+dP/dt$ reaches maximum in 1–2 minutes followed by decline in WT but not PLM-KO hearts.[20] In addition, expressing the phosphomimetic PLM S68E mutant (inhibits NCX1 but not NKA)[20,24] in PLM-KO hearts resulted in higher $+dP/dt$ in response to isoproterenol when compared to PLM-KO hearts expressing green fluorescent protein, suggesting NCX1 inhibition by phosphorylated PLM results in enhancement of cardiac contractility.[25] These observations suggest that PLM, when phosphorylated at serine68 under catecholamine stress, minimizes risks of arrhythmogenesis but preserves cardiac contractility. Therefore, regulation of PLM expression and its phosphorylation may be important for protection against stress-induced arrhythmia. We hypothesized that this mechanism may be of particular importance post–myocardial infarction (MI).

In 2000, Sehl et al. reported that PLM mRNA increases twofold as early as 3 days after MI in the rat and remains elevated for at least 2 weeks.[26] In adult rat ventricles, PLM protein levels are elevated fourfold 7 days post-MI.[9] This study was undertaken to evaluate the role of PLM on contractility and survival in ischemic cardiomyopathy, using WT and PLM-KO mice generated in our lab[8,27] for both *in vivo* and *in vitro* studies.

Methods

Generation of PLM-deficient mice and animal care

A mouse line deficient in PLM was generated by replacing exons 3–5 of the PLM gene with lacZ and neomycin resistance genes, as described in detail previously.[8] A panel of informative mapped microsatellite loci was used to generate congenic animals on the C57BL/6 genetic background using a "speed congenic" strategy. C57BL/6 animals with an unmodified PLM gene were used as controls.

WT and PLM-KO cohorts used for this study were age and sex matched. Only male animals were used, the mean age being 16 weeks. Mice were housed in a vivarium supervised by

[1]Cardiovascular Division, Department of Medicine; [2]Cardiovascular Research Center; [3]Department of Biomedical Engineering; [4]Department of Pediatrics, University of Virginia Medical Center, Charlottesville, Virginia, USA; [5]Division of Nephrology and Center of Translational Medicine, Department of Medicine, Thomas Jefferson University, Philadelphia, Pennsylvania, USA; [6]Department of Molecular Physiology and Biological Physics, University of Virginia Medical Center, Charlottesville, Virginia, USA.

Correspondence: Joseph Y. Cheung (joseph.cheung@jefferson.edu)

DOI: 10.1111/j.1752-8062.2012.00403.x

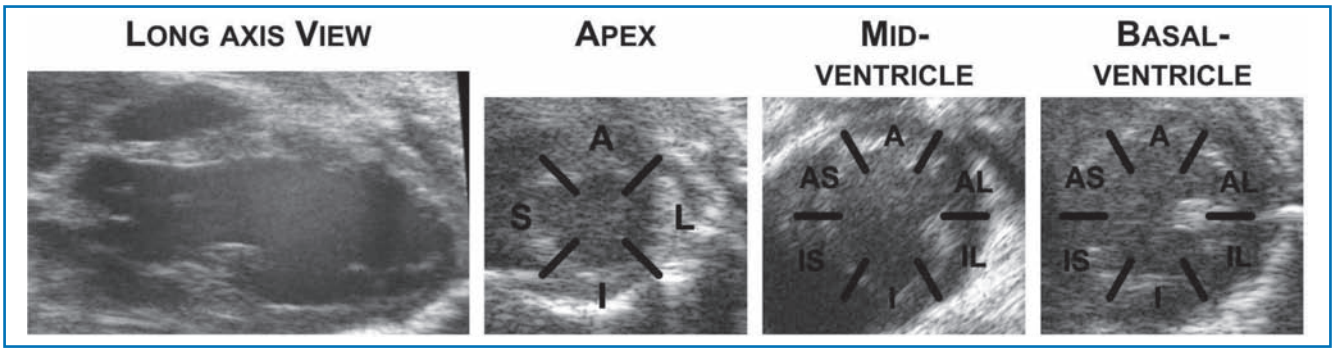

Figure 1. A 16-segment model used for calculation of the wall motion score index. Long-axis (left panel) and short-axis (right three panels) views at the level of apex, mid-ventricle and basal-ventricle were obtained. (A = Anterior; AL = Anterolateral; IL = Inferolateral; I = Inferior; IS = Inferoseptal; AS = Anteroseptal).

the Department of Comparative Medicine at the University of Virginia Health Sciences Center. Standard care was provided to all mice used for experiments. All protocols applied to the mice in this study were approved and supervised by Institutional Animal Care and Use Committees at the University of Virginia, the Pennsylvania State University College of Medicine, and the Thomas Jefferson University.

Induction of MI

Mice were anesthetized by pentobarbital (100 mg/kg i.p.) and body temperature was maintained at 37°C. Electrocardiographic (ECG) leads were attached to the limbs. After endotracheal intubation, mice were ventilated with 100% oxygen. The heart was exposed through an incision between the left third and fourth ribs and the left anterior descending artery was identified and ligated. Myocardial ischemia was confirmed by blanching of the myocardium and ECG changes of ST segment elevation. Buprenorphine was given subcutaneously for postoperative analgesia. Sham operations were identical except that the coronary artery was not ligated.

Echocardiography

Three weeks after sham or MI surgery, mice were anesthetized with isoflurane (1.5–3%) and oxygen (97–98.5%) via facemask. Animals were placed supine on a heating pad to maintain body temperature and their limbs were attached to electrodes. Hair on the chest was depilated and prewarmed aquasonic gel applied to the precordium. Transthoracic echocardiography was performed using a Vevo770 ultrasound system (Visualsonics, Toronto, Canada) equipped with a 35-MHz probe. Two-dimensional images were obtained by gating to the ECG to trigger signal acquisition (ECG-based Kilohertz Visualization, EKV). Two-dimensional parasternal long-axis and short-axis images were acquired and stored as digital loops. The parasternal long-axis view was used for calculation of left ventricular (LV) ejection fraction (EF), LV fractional area of contraction (FAC), LV end systolic volume (LVVs), and LV end-diastolic volume (LVVd). The system software uses a formula based on cylindrical hemi-elliptoid model to measure volumes (volume = $4\pi/3 \times$ LV area/2[LV area/π(LV major/2]). It further uses LVVs and LVVds to calculate EF and FAC. The parasternal short-axis images at the apex, mid-ventricle, and base of the LV were used to calculate a wall motion score index. A 16-segment model based on that described by the American Society of Echocardiography was used to compute the score (*Figure 1*). According to this model, the apex is divided into four segments, and the mid-ventricle and the base of the ventricle into six segments each. Wall motion is scored as 1 = Normal, 2 = Hypokinetic, 3 = Akinetic, 4 = Dyskinetic, and 5 = Aneurysmal. The ratio of the sum of all wall motion scores to all segments scored was calculated.

Histopathological analysis

Animals were weighed and euthanized by CO_2 overdose on day 21 after MI. After excision, hearts were rinsed in phosphate-buffered saline (PBS), weighed, fixed in 10% zinc formalin overnight, and embedded in paraffin. Sections (3 μm) were cut transversely approximately every 1 mm from the apex to the base of the heart, and stained with Masson's trichrome stain to identify the infarcted myocardium. The infarct region was measured at three levels (apex, mid, and base) using Imagepro Plus software. Infarct size was expressed as the percent of the total summed LV circumferential length represented by the summed infarct size.

Isolation of adult murine cardiac myocytes

Postinfarction myocytes were isolated from the septum and LV free wall of WT and PLM-KO mice as described by Zhou et al.[28] and modified by us.[20,24,27] Infarct scar and the area in sham-operated hearts corresponding to infarct scar in post-MI hearts were excised before final enzymatic digestion step. Myocytes were used within 2–8 hours of isolation.

Myocyte shortening measurements

Myocytes adherent to coverslips were bathed in 0.6 mL of air- and temperature-equilibrated (37°C), N-2-hydroxyethylpiperazine-N-2-ethanesulfonic acid (HEPES)-buffered (20 mM, pH 7.4) medium 199 containing 0.6, 1.8 or 5.0 mM $[Ca^{2+}]_o$. Measurements of myocyte contraction (1 Hz) were performed as previously described.[20,24,27]

$[Ca^{2+}]_i$ transient measurements

Myocytes were exposed to 0.67 μM of fura-2 AM for 15 minutes at 37°C. Fura-2 loaded myocytes were field-stimulated to contract (1 Hz, 37°C) in medium 199 containing 0.6, 1.8, or 5.0 mM $[Ca^{2+}]_o$ $[Ca^{2+}]_i$ transient measurements, daily calibration of fura-2 fluorescent signals, and $[Ca^{2+}]_i$ transient analyses were performed as previously described.[20,24,27]

NCX1 current (I_{NaCa}) measurements

Whole cell patch-clamp recordings were performed at 30°C as previously described.[12,20,27] Briefly, fire-polished pipettes with resistances of 0.8–1.4 M when filled with standard internal solution were used. Pipettes were filled with a buffered Ca^{2+} solution containing (in mM) 100 Cs^+ glutamate, 7.25 Na-HEPES,

	WT-sham	WT-MI	KO-sham	KO-MI
Body Weight (BW) (g)	28.4 ± 1.2 (7)	27.8 ± 0.8 (16)	27.7 ± 0.5 (16)	28.3 ± 0.4 (15)
Heart Weight (HW) (mg)	149 ± 10	183 ± 4[a]	146 ± 5	183 ± 5[a]
HW/BW (mg/g)	5.23 ± 0.20	6.64 ± 0.18[a]	5.26 ± 0.10	6.46 ± 0.13[a]
HW/Tibial Length (mg/mm)	67.5 ± 2.4	82.6 ± 0.9[a]	63.2 ± 1.3	78.9 ± 3.3[a]
C_m, pF	150 ± 5 (29)	187 ± 7[a] (17)	166 ± 8 (27)	214 ± 9[a,b] (10)

Values are means ± SE; numbers in parentheses are numbers of observations.
[a]$p < 0.002$ (WT-sham vs. WT-MI or KO-sham vs. KO-MI); [b]$p < 0.025$ (WT-MI vs. KO-MI).

Table 1 Effects of PLM knockout and MI on heart weight and C_m.

1 $MgCl_2$, 12.75 HEPES, 2.5 Na_2ATP, 10 EGTA, and 6 $CaCl_2$; pH 7.2. Free Ca^{2+} in the pipette solution was approximately 205 nM, determined fluorimetrically with fura-2. Myocytes were bathed in an external solution containing (in mM) 130 NaCl, 5 CsCl, 1.2 $MgSO_4$, 1.2 NaH_2PO_4, 5 $CaCl_2$, 10 HEPES, 10 Na^+-HEPES, and 10 glucose; pH 7.4. Verapamil (1 μM), ouabain (1 mM), and niflumic acid (10 μM) were used to block L-type Ca^{2+}, Na^+-K^+-ATPase, and Cl^- currents, respectively. K^+ currents were minimized by Cs^+ substitution for K^+ in both pipette and external solutions. After break-in, membrane potential was held at the theoretical reversal potential (–73 mV) of I_{NaCa} for 5 minutes before onset of voltage ramp. This precaution minimized ion fluxes through NCX1 before the voltage ramp and allowed $[Na^+]_i$ and $[Ca^{2+}]_i$ to equilibrate with those present in pipette solution. A descending voltage ramp (from +100 to –120 mV; 500 mV/s) followed by an ascending voltage ramp (from –120 to +100mV; 500 mV/s) was applied, and repeated after addition of 1mM $CdCl_2$ to the external solution. Currents (filtered at 1 kHz, digitized at 2 kHz) were derived from measurements during the descending voltage ramp. I_{NaCa} was defined as the difference current measured in the absence and presence of Cd^{2+}, and normalized to whole cell capacitance (C_m) to facilitate comparison of I_{NaCa} between WT and PLM-KO myocytes. Our ionic conditions were biased toward measurement of reverse Na^+/Ca^{2+} exchange (outward current).

PLM immunoblotting

Left ventricles were excised, rinsed in ice-cold PBS, and cut into small pieces. For MI hearts, the infarct scar was excised prior to tissue homogenization. For sham hearts, the area corresponding to the scar in infarct hearts was excised and discarded. Approximately, 60 mg of tissue were suspended in 700 μL of ice-cold lysis buffer containing (in mM) 50 Tris (pH 8.0), 150 NaCl, 1 Na^+ orthovanadate, 1 phenylmethylsulfonyl fluoride (PMSF), 100 NaF, 1 ethyleneglycol bis(2-aminoethylether)-N,N,N,N-tetracetic acid (EGTA), and 0.5% NP40. A protease inhibitor cocktail tablet (Penzberg, Germany) was also added to 10 mL of lysis buffer. The tissue was homogenized with a glass dounce homogenizer (15–20 strokes), placed on ice for 15 minutes, before centrifugation at 20,800 g for 10 minutes at 4°C. The supernatant was snap-frozen with dry ice-ethanol and stored at –80°C.

Proteins in heart homogenates were subjected to 12% sodium dodecyl sulfate polyacrylamide gel electrophoresis (SDS-PAGE) under reducing (5% β-mercaptoethanol) conditions. The fractionated proteins were transferred onto ImmunBlot polyvinylidene difluoride (PVDF) membranes. Primary antibodies used for unphosphorylated PLM were polyclonal antibody C2 (1:10,000) and for PLM phosphorylated at Ser68 polyclonal antibody CP68 (1:1,000). Secondary antibodies used were donkey anti-rabbit IgG (Amersham; Piscataway, NJ, USA). Immunoreactive proteins were detected with an enhanced chemiluminescence Western blotting system. Protein band signal intensities were quantitated by scanning autoradiograms of the blots with a phosphorimager (Molecular Dynamics; Sunnyvale, CA, USA).

Statistics

All results are expressed as means ± SE. For analysis of a parameter (e.g., maximal contraction amplitude) as functions of group (WT-sham, WT-MI, PLM-KO-MI) and $[Ca^{2+}]_o$, two-way ANOVA was used to determine statistical significance. Two-way ANOVA was also used to analyze I_{NaCa} as a function of group and membrane voltage. For analysis of PLM abundance, membrane capacitance, and echocardiographic indices, one-way ANOVA was used. A commercial software package (JMP version 4.05; SAS Institute, Cary, NC, USA) was used. In all analyses, $p < 0.05$ was taken to be statistically significant.

Results

Effects of PLM-KO and MI on heart weight and myocyte size

There were no differences in body weight between WT and PLM-KO mice (*Table 1*; group effect, $p = 0.86$), regardless of whether the mice had undergone sham or MI operation (*Table 1*; MI effect, $p = 0.98$). Heart weight, heart weight/body weight, and heart weight/tibial length were not different between WT and PLM-KO mice (*Table 1*; group effect, $p = 0.76$, 0.71, and 0.20, respectively). Induction of MI significantly increased heart weight, heart weight/body weight, and heart weight/tibial length in both WT and PLM-KO mice (*Table 1*; MI effect, $p < 0.0001$ for all three parameters). Lack of significant group × MI interaction effect indicates that MI did not result in larger increases in PLM-KO heart weights ($p = 0.76$), and heart weights normalized to body weights ($p = 0.59$) or tibial lengths ($p = 0.91$).

Whole cell capacitance (C_m), a measure of myocyte surface area and therefore an estimate of cell size, was not different between WT and PLM-KO myocytes (*Table 1*; $p = 0.11$). Induction of MI caused significant increases in C_m in both WT and PLM-KO myocytes (*Table 1*; $p < 0.002$). Post-MI, myocytes isolated from PLM-KO hearts were significantly larger than those isolated from WT hearts (*Table 1*; $p < 0.025$).

Effects of PLM-KO and MI on survival and *in vivo* cardiac function

WT mice suffered approximately 30% mortality at 3 weeks post-MI (*Figure 2*), consistent with the peri-infarct mortality reported for this strain of mouse.[29] By contrast, mortality was approximately 50% in PLM-KO mice post-MI (*Figure 2*). Interestingly, WT

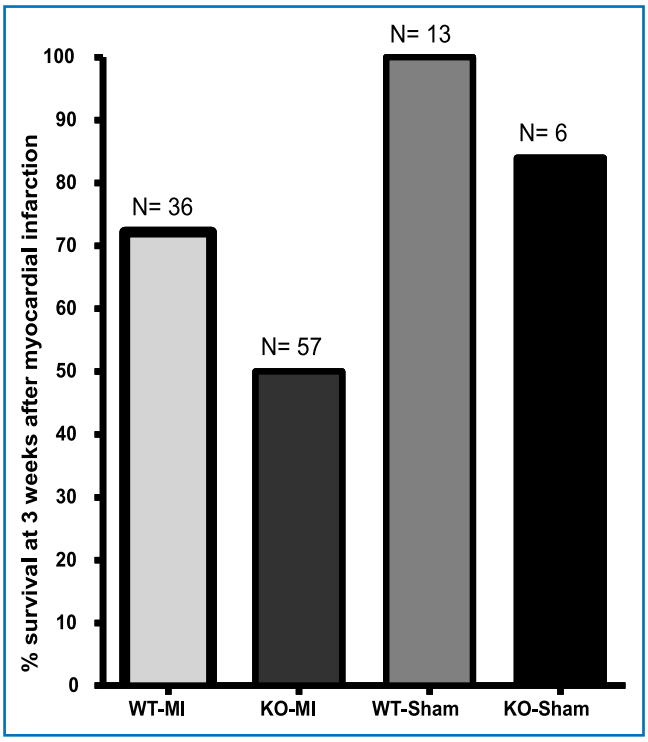

Figure 2. Survival in PLM deficient and WT animals after 3 weeks of sham or MI operation.

	WT-sham	WT-MI	KO-sham	KO-MI
EF (%)	64.2 ± 4.4	20.8 ± 1.7[a]	73.4 ± 5.5[b]	42.4 ± 4.6[a,b]
FAC (%)	42.8 ± 3.9	11.8 ± 1.7[a]	53.8 ± 5.8[b]	26.7 ± 3.6[a,b]
LVVs	21.1 ± 2.8	80.7 ± 10.6[a]	15.3 ± 4.4[b]	38.2 ± 6.1[a,b]
LVVd	58.2 ± 1.8	101.4 ± 12.3[a]	54.0 ± 6.2	65.5 ± 7.3[a]
WM score	1.0	2.16 ± 0.08[a]	1.0	1.63 ± 0.09[a,b]

Values are means ± SE; sham groups: $n = 5$; MI groups: $n = 9$.
EF = ejection fraction; FAC = fractional area contraction; LVVs = left ventricular end-systolic volume; LVVd = left ventricular end-diastolic volume; WM = wall motion.
[a]$p < 0.0001$ (WT-sham vs. WT-MI or KO-sham vs. KO-MI); [b]$p < 0.01$ (WT-sham vs. KO-sham or WT-MI vs. KO-MI).

Table 2 Effects of PLM knockout and MI on *in vivo* cardiac function.

animals that underwent sham operation had no mortality but PLM-KO-sham mice suffered approximately 16% mortality. This suggests that PLM-deficient mice did not tolerate surgical stress well. Infarct sizes were not significantly different between the two groups (*Figure 3*, $p = 0.21$). This observation indicates that larger infarct size leading to severe heart failure is unlikely to account for the increased mortality observed in PLM-KO-MI animals.

As a group, PLM-KO mice had significantly higher EFs and FAC, and lower LVVs when compared to WT mice (*Table 2*), regardless of whether they had suffered MI (group effect, $p < 0.01$). Induction of MI significantly lowered the EF and FAC and increased LVVs and LVVd in both WT and PLM-KO hearts (MI effect, $p < 0.02$). Post-MI, EF, FAC, and LVVs were significantly ($p < 0.01$) higher whereas wall motion abnormalities were significantly less in PLM-KO hearts when compared to WT hearts ($p < 0.004$).

Effects of PLM-KO and MI on myocyte contraction

Our previous studies[30] demonstrated that when extracellular Ca^{2+} concentration ($[Ca^{2+}]_o$) was varied to manipulate the thermodynamic driving force for NCX1, myocytes isolated from rat hearts 3 weeks post-MI displayed steady-state contraction amplitudes that were higher at 0.6, similar at 1.8 and lower at 5.0 mM $[Ca^{2+}]_o$ when compared to myocytes isolated from sham-operated rats. This observation is consistent with suppressed NCX1 activity in post-MI rat myocytes.[31] In WT mice, myocytes that have survived a moderate size (30–35%) infarct also shortened more at 0.6, similarly at 1.8 and less at 5.0 mM $[Ca^{2+}]_o$ when compared to WT-sham myocytes (*Figure 4*; *Table 3*). Two-way ANOVA showed absence of group ($p = 0.66$) but strong group × $[Ca^{2+}]_o$ ($p < 0.012$) interaction effects, indicating that manipulating $[Ca^{2+}]_o$ had different effects on cell shortening between WT-sham and WT-MI myocytes. Similarly, strong group × $[Ca^{2+}]_o$ interaction effects were observed for maximal shortening ($p < 0.005$) and maximal relengthening velocities ($p < 0.009$).

Compared to WT-MI myocytes, myocytes isolated from PLM-KO hearts 3 weeks post-MI shortened significantly less at 0.6 and more at 5.0 mM $[Ca^{2+}]_o$ (*Figure 4*; *Table 3*; group × $[Ca^{2+}]_o$ effect, $p < 0.02$). Maximal shortening ($p < 0.018$) and relengthening ($p < 0.014$) velocities were also lower at 0.6 but higher at 5.0 mM $[Ca^{2+}]_o$ in PLM-KO-MI when compared to WT-MI myocytes (*Table 3*). It appears as if the deleterious effects of MI on myocyte contractility were ameliorated by the absence of PLM. Indeed, comparing PLM-KO-MI with WT-sham myocytes, there were no differences in contraction

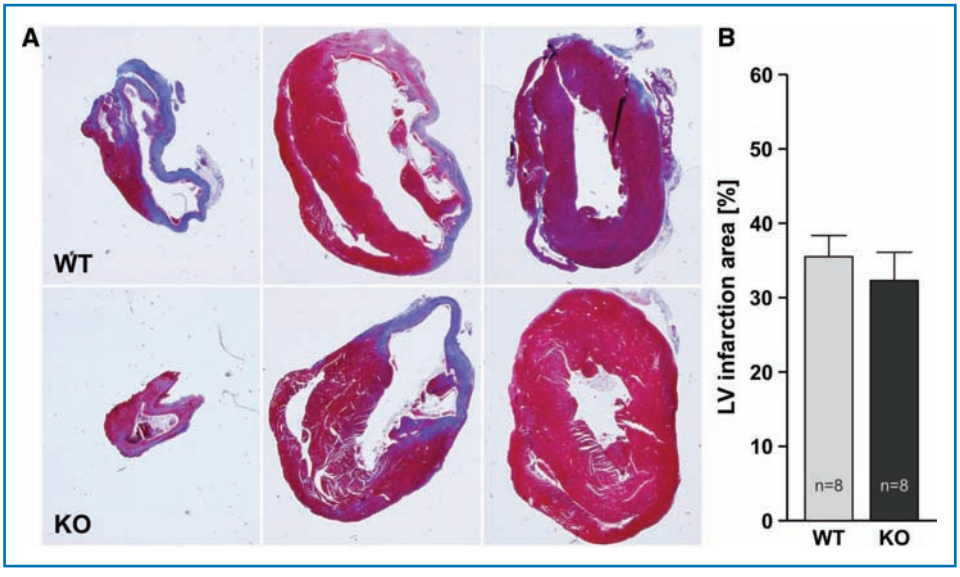

Figure 3 (A) Representative image of trichrome Masson staining of infarcted left ventricle from WT and PLM-KO mice showing fibrosis of infarcted myocardium (photographed at 10X magnification. (B) Comparison of infarct size between PLM-KO and WT mice ($p = 0.21$).

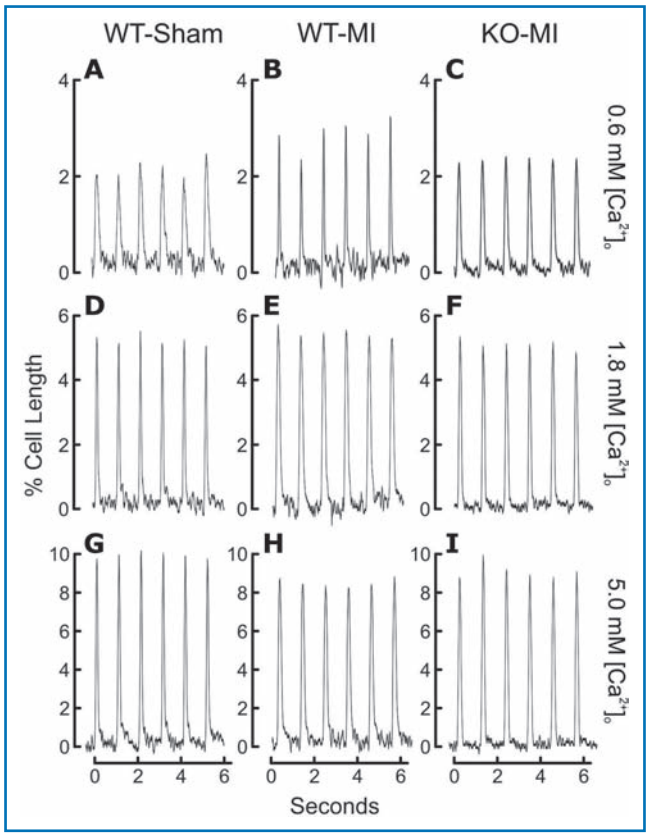

Figure 4 Myocytes contractility of WT-sham, WT-MI, and KO-MI under different extracellular Ca^{2+} concentration ($[Ca^{2+}]_o$). Isolated myocytes were paced (1 Hz) to contract at 37°C and $[Ca^{2+}]_o$ of 0.6 (A–C), 1.8 (D–F) or 5.0 mM (G–I). Shown are steady-state paced twitches from myocytes harvested from WT-sham (*A, D, G*), WT-MI (*B, E, H*) and WT-KO (*C, F, I*) hearts. Composite results are summarized in Table 3.

$[Ca^{2+}]_o$	WT-sham	WT-MI	KO-MI
	Maximal contraction amplitude (% of resting cell length)		
0.6	2.19 ± 0.15 (18)	2.74 ± 0.26[a] (22)	2.21 ± 0.18 (31)
1.8	5.57 ± 0.36 (17)	5.62 ± 0.25 (29)	5.38 ± 0.29 (31)
5.0	9.99 ± 0.43 (22)	8.45 ± 0.40[a] (27)	9.54 ± 0.53 (38)
	Maximal shortening velocity (cell length/s)		
0.6	0.30 ± 0.05	0.52 ± 0.05[a]	0.42 ± 0.03
1.8	0.86 ± 0.07	0.86 ± 0.05	0.87 ± 0.06
5.0	1.51 ± 0.08	1.25 ± 0.07[a]	1.46 ± 0.09
	Maximal relengthening velocity (cell length/s)		
0.6	0.21 ± 0.03	0.35 ± 0.04[a]	0.30 ± 0.03
1.8	0.67 ± 0.08	0.70 ± 0.06	0.69 ± 0.05
5.0	1.29 ± 0.08	1.02 ± 0.07[a]	1.28 ± 0.09

Values are means ± SE; numbers in parentheses are pooled numbers of myocytes from three WT-sham, four WT-MI, or six PLM-KO-MI hearts. There are no differences in the measured parameters between WT-sham and PLM-KO-MI myocytes.
[a]$p < 0.02$ (WT-MI vs. WT-sham).

Table 3 Effects of PLM knockout and MI on myocyte contractility.

$[Ca^{2+}]_o$	WT-MI	KO-MI
	Systolic $[Ca^{2+}]_i$ (nM)	
0.6	175 ± 6 (30)	152 ± 4[a] (20)
1.8	252 ± 9 (30)	266 ± 9 (26)
5.0	307 ± 11 (34)	379 ± 16[a] (30)
	Diastolic $[Ca^{2+}]_i$ (nM)	
0.6	87 ± 5	89 ± 4
1.8	110 ± 5	119 ± 5
5.0	123 ± 5	117 ± 6
	Increase in fluorescence intensity ratio (%)	
0.6	18.7 ± 0.7	13.5 ± 0.8[a]
1.8	26.1 ± 0.7	26.4 ± 1.2
5.0	30.9 ± 0.8	42.8 ± 1.4[a]
	$t_{1/2}$ of $[Ca^{2+}]_i$ decline (ms)	
0.6	206 ± 8	217 ± 15
1.8	161 ± 8	169 ± 9
5.0	154 ± 6	132 ± 7

Values are means ± SE; numbers in parentheses are pooled number of myocytes from five WT-MI and five PLM-KO-MI hearts.
[a]$p < 0.0001$.

Table 4 Effects of PLM knockout and MI on $[Ca^{2+}]_i$ transients.

amplitude ($p = 0.54$), maximal shortening ($p = 0.31$), and relengthening ($p = 0.58$) velocities.

Effects of PLM-KO and MI on $[Ca^{2+}]_i$ transients

Compared to WT-MI myocytes, systolic $[Ca^{2+}]_i$ was lower at 0.6, not different at 1.8, and higher at 5.0 mM $[Ca^{2+}]_o$ in PLM-KO-MI myocytes (*Table 4*). This conclusion is supported by strong group × $[Ca^{2+}]_o$ interaction effect ($p < 0.0001$). Across the range of $[Ca^{2+}]_o$ examined, there were no differences in diastolic $[Ca^{2+}]_i$ between WT-MI and PLM-KO-MI myocytes ($p = 0.3$). Therefore, it is to be expected that the $[Ca^{2+}]_i$ transient amplitudes would be lower at 0.6 and higher at 5.0 mM $[Ca^{2+}]_o$ in PLM-KO-MI myocytes. Indeed, this is the case as reflected by the percent increase in fura-2 fluorescence intensity ratio (*Table 4*; group × $[Ca^{2+}]_o$ interaction effect, $p < 0.0001$), an estimate of $[Ca^{2+}]_i$ transient amplitude that is independent of fura-2 fluorescence calibration procedures.

The $t_{1/2}$ of $[Ca^{2+}]_i$ decline, an estimate of rate of SR Ca^{2+} uptake,[32] was similar between WT-MI and PLM-KO-MI myocytes.

Effects of PLM-KO and MI on Na^+/Ca^{2+} exchange current (I_{NaCa})

We and others have previously demonstrated that post-MI, NCX1 activity is depressed in rat cardiac myocytes.[31,33] In addition, myocyte contraction abnormalities post-MI can be rescued by overexpression of NCX1.[34] PLM is known to inhibit the activity of NCX1 in the heart.[10] We therefore tested the hypothesis that the salutatory effects of PLM deficiency on post-MI contractility and $[Ca^{2+}]_i$ homeostasis are due to relief of inhibition of NCX1 by PLM. In agreement with our previous findings on rat myocytes,[31] I_{NaCa} was significantly (group × voltage effect, $p < 0.0001$) lower in WT-MI when compared to WT-sham myocytes (*Figure 5*). PLM deficiency significantly ($p < 0.0001$) increased I_{NaCa} in post-MI myocytes when compared to WT-MI myocytes.

Effects of PLM-KO and MI on PLM expression and phosphorylation

In contrast to previous reports that PLM was increased in rat hearts 1 week post-MI,[9,26] we observed significant ($p < 0.05$)

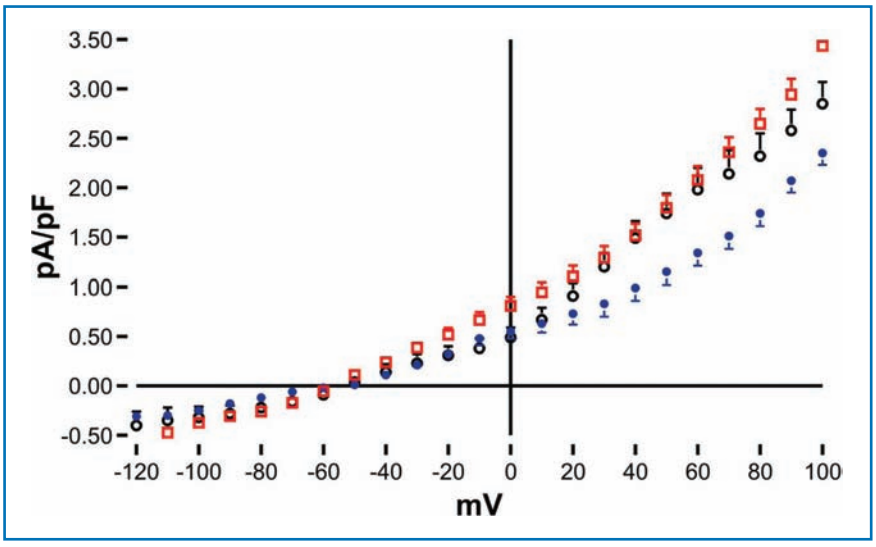

Figure 5 Current–voltage relationships of Na^+/Ca^{2+} exchange current (I_{NaCa}) in WT-MI and KO-MI myocytes. I_{NaCa} was measured at 5mM $[Ca^{2+}]_o$ and 30°C with a descending–ascending voltage-ramp protocol as described in "Methods." Free $[Ca^{2+}]$ in the Ca^{2+}-buffered pipette solution was 205 nM. Holding potential was at the calculated reversal potential of I_{NaCa} (–73 mV) under our experimental conditions. There were 7 WT-sham (open circles), 10 WT-MI (filled circles), and 10 KO-MI (open squares). Errors bars are not drawn if they fall within the boundaries of the symbol. Two-way ANOVA indicates significantly lower I_{NaCa} in WT-MI when compared to WT-sham (group, $p < 0.0001$; group × voltage interaction, $p < 0.0001$) or to KO-MI myocytes (group, $p < 0.0001$; group × voltage interaction, $p < 0.0001$). I_{NaCa} magnitudes are higher in KO-MI when compared to WT-sham myocytes (group, $p < 0.002$; group × voltage interaction, $p < 0.002$).

reduction of unphosphorylated PLM in 3-week post-MI (21.2 ± 3.4 arbitrary units; $n = 7$) compared to sham (41.2 ± 4.0 arbitrary units; $n = 9$) mouse hearts. PLM phosphorylated at Ser68 was significantly ($p < 0.05$) increased in post-MI (61.5 ± 13.1 arbitrary units; $n = 7$) compared to sham (31.4 ± 1.8 arbitrary units; $n = 6$). As expected, we could not detect any PLM in PLM-KO hearts.

Discussion

Under resting conditions, baseline $[Na^+]_i$,[18,20] cardiac output and myocyte contraction (1.8 mM $[Ca^{2+}]_o$, 1–2 Hz)[20,27] are similar between WT and PLM-KO hearts. Therefore, PLM is functionally quiescent in resting myocytes. When animals are under stress with high catecholamine levels, PLM is phosphorylated at serine68. Phosphorylated PLM relieves its tonic inhibition on NKA, thereby minimizing Na^+ and Ca^{2+} overload in cardiac cells.[20,23] Simultaneously, phosphorylated PLM, via its action on NCX1,[22] preserves inotropy.[25] These considerations led to the concept that PLM is a cardiac stress protein, i.e., its functional significance is manifest only when the animal or myocyte is under duress.[35] To test this hypothesis, we induced MI in WT and PLM-KO mice to evaluate whether the absence of PLM is beneficial or detrimental. The major finding is that while PLM deficiency resulted in enhanced EF and myocyte contractility and improved $[Ca^{2+}]_i$ homeostasis post-MI, absence of PLM was detrimental to whole animal survival post-MI. Viewed in this context, the stress protein PLM needed to be present post-MI to minimize risks of sudden death, at the cost of reduced inotropy.

Our MI mouse model exhibited many of the pathological changes observed in post-MI myocytes of other species. For example, as we have observed in the rat,[36] post-MI murine myocytes were hypertrophied, as evidenced by increases in heart weight/body weight ratio and whole cell capacitance. The contractile phenotype observed in post-MI mouse myocytes was also similar to that seen in rat myocytes.[30] Similar to post-MI rabbit[37] and rat[31] cardiac myocytes, I_{NaCa} was depressed in mouse myocytes 3 weeks post-MI. In contrast to the increase in PLM mRNA and protein levels following MI in rat hearts,[9,26] we observed a decrease in PLM expression, accompanied by an increase in the fraction of phosphorylated PLM in murine hearts 3 weeks post-MI. Increased phosphorylation accompanied by decreased expression of PLM was also observed in a rabbit heart failure model.[38] Increased fractional phosphorylation of PLM post-MI may account for the decreased I_{NaCa} observed in WT-MI myocytes.

In cardiac myocytes, there are three major ion transport systems that regulate $[Ca^{2+}]_i$. MI is not known to grossly distort L-type Ca^{2+} currents.[39] Therefore, it appears unlikely that changes in L-type Ca^{2+} channels mediate the improvement in contractility in PLM-KO-MI myocytes. Post-MI, sarcoplasmic reticulum (SR) Ca^{2+} uptake activity, as reflected by $t_{1/2}$ of $[Ca^{2+}]_i$ decline,[32] was not different between WT-MI and PLM-KO-MI myocytes. Therefore, improvement in cardiac function in PLM-KO myocytes post-MI was unlikely due to increased SR Ca^{2+} uptake activity. The role of increased SR Ca^{2+} leak in mediating reduced contractility in heart failure remains controversial.[40,41] We did not detect increased SR Ca^{2+} leak in post-MI rat myocytes.[32] NCX1 activity, however, was clearly enhanced in PLM-KO-MI myocytes when compared to WT-MI myocytes and likely accounted for the improvement in cardiac contractility based on the following considerations. First, the pattern of contractile and $[Ca^{2+}]_i$ transient abnormalities observed in post-MI myocytes (higher at 0.6, not different at 1.8, but lower at 5.0 mM $[Ca^{2+}]_o$) mimicked that in normal rat myocytes in which NCX1 was downregulated by antisense,[42] and was exactly the opposite to that found in NCX1 overexpressed myocytes.[43] Second, contractile abnormalities in post-MI myocytes could be rescued by NCX1 overexpression.[45] Third, NCX1 was shown to contribute significantly to maintenance of contractile function and $[Ca^{2+}]_i$ transients in failing human ventricular myocytes.[44–46] Fourth, in animal models, heterozygous transgenic overexpression of NCX1 in mice has been demonstrated to attenuate ischemic and hypoxic contractile dysfunction *in vitro*[47] and to improve post-MI myocardial function *in vivo*.[48] Mechanistically, the elevated $[Na^+]_i$ and prolonged action potential duration in post-MI myocytes[49] would favor Ca^{2+} influx via NCX1 operating in the reverse mode, thereby directly contributing to SR Ca^{2+} filling[50] and improved myocyte contractility.

It has been reported that increased fibrosis is present in PLM-KO compared to WT hearts.[20] A possible explanation for the improved cardiac performance in PLM-KO-MI compared to WT-MI hearts is that the increased fibrosis in noninfarct tissue reduces functional expansion of the infarct and accounts for better *in vivo* indices of LV function. Although this hypothesis is attractive, it fails to account for the improvement in contractility and $[Ca^{2+}]_i$ homeostasis in PLM-KO-MI compared to WT-MI myocytes.

Despite improved pump performance in PLM-KO mice post-MI, perioperative survival was clearly decreased when compared to WT-MI mice. The lifespan of PLM-KO mice is

not different than that of WT mice.[8] Under high catecholamine states, relief of inhibition of NKA by PLM attenuates cellular Na^+ and Ca^{2+} overload and minimizes risks of arrhythmogenesis.[20,23] Loss of regulation of NKA in PLM-KO-MI myocytes would lead to inexorable increases in $[Na^+]_i$,[20,23] resulting in increased spontaneous activity and perhaps sudden death. In addition, both MI[49] and PLM deficiency,[27] each by itself, can cause prolongation of action potential duration which is known to engender increased arrhythmias. If the effects of MI and PLM deficiency are additive in terms of action potential prolongation, then increased risk of sudden death is to be expected. Another explanation is that increased forward Na^+/Ca^{2+} exchange to pump Ca^{2+} out during diastole may result in more after-depolarization in PLM-KO-MI myocytes, resulting in increased arrhythmogenesis. Increased NCX1 activity in a rabbit model of heart failure has been suggested to be pathogenic in arrhythmogenesis.[51] Finally, increased fibrosis in PLM-KO hearts,[20] especially if near the border zone, may engender a greater propensity for reentrant arrhythmias resulting in increased mortality.

In our present and previous studies,[31,52] we observed that I_{NaCa} was decreased in post-MI rodent myocytes. In post-MI rabbit myocytes, I_{NaCa} was also decreased, although NCX1 protein levels were increased.[37] To provide a balanced view, however, we wish to note that in some animal models, I_{NaCa} was increased rather than decreased post-MI.[53,54] In other models of nonischemic heart failure including human end-stage cardiomyopathy, NCX1 was either decreased, unchanged, or increased.[55] The reasons why NCX1 was decreased in some models of heart failure but increased in others are not obvious, but may relate to different experimental models (e.g., post-MI vs. rapid pacing vs. valvular defects), species differences (rat vs. rabbit), presence or absence of overt heart failure, and different stages of disease at which myocyte function was examined. In addition, with few exceptions,[9,38] levels of PLM or its fractional phosphorylation were not evaluated in experimental heart failure models. Differences in PLM expression or its phosphorylation may account for the apparent discrepancies in NCX1 activity in different models of heart failure.

There are some limitations to this study. The first is that unlike PLM-KO mice of mixed genetic background,[8] PLM-KO mice backcrossed to a pure congenic C57BL/6 background had similar resting EF and cardiac output when compared to their WT littermates.[20,56] In this study, KO-sham mice had higher EF and FAC when compared to WT-sham mice. This difference may be due to residual stress of the open chest operation. Higher catecholamine levels would result in higher $+dP/dt$ in PLM-KO mice in the postoperative period.[20] The second apparent discrepancy is that while inhibition of NCX1 by PLM-S68E mutant expressed in PLM-KO hearts resulted in enhancement of contractility,[25] our present data suggest that enhanced NCX1 activity largely accounted for the improvement in cardiac and myocyte contractility in PLM-KO-MI hearts as compared to WT-MI hearts. We submit, however, that there is no discrepancy. In WT myocytes and PLM-KO myocytes expressing PLM-S68E mutant, action potential duration is quite brief and $[Na^+]_i$ relatively low.[25] These prevailing conditions favor Ca^{2+} efflux by forward Na^+/Ca^{2+} exchange during an excitation–contraction (EC) cycle. Therefore, inhibition of NCX1 by phosphorylated PLM would result in less Ca^{2+} efflux and increased inotropy. Post-MI, action potential duration is prolonged[49] and $[Na^+]_i$ is higher: both conditions favor Ca^{2+} influx by reverse Na^+/Ca^{2+} exchange. Enhanced NCX1 activity in PLM-KO-MI myocytes would be expected to increased SR Ca^{2+} filling during an EC cycle and contribute to improved contractility.

In summary, genetically engineered PLM deficiency resulted in increased postoperative mortality, but enhanced cardiac performance in survivors of surgically induced MI. Improved cardiac and myocyte contractility in PLM-deficient mice postinfarction was likely due to changes in cellular Ca^{2+} homeostasis mediated by enhanced Na^+/Ca^{2+} exchange activity. Higher mortality in PLM-deficient mice postinfarction may be due to lack of regulation of NKA activity by PLM, and prolonged action potential duration. We suggest both Na^+/Ca^{2+} exchange and NKA activities need to be exquisitely regulated after infarction to balance the deleterious effects of increased arrhythmogenesis and the beneficial effects of enhanced myocyte contractility.

Acknowledgments

This study was supported in part by National Institutes of Health Grants RO1-HL-58672 (JYC), RO1-HL-74854 (JYC), RO1-HL-69074 (ALT), T32-HL007355–26 Training Grant (MAM), and by an institutional grant from the Cardiovascular Research Center at the University of Virginia (ALT).

References

1. Presti CF, Scott BT, Jones LR. Identification of an endogenous protein kinase C activity and its intrinsic 15-kilodalton substrate in purified canine cardiac sarcolemmal vesicles. *J Biol Chem.* 1985; 260: 13879–13889.

2. Sweadner KJ, Rael E. The FXYD gene family of small ion transport regulators or channels: cDNA sequence, protein signature sequence, and expression. *Genomics.* 2000; 68: 41–56.

3. Attali B, Latter H, Rachamim N, Garty H. A corticosteroid-induced gene expressing an "IsK-like" K^+ channel activity in Xenopus oocytes. *Proc Natl Acad Sci USA.* 1995; 92: 6092–6096.

4. Morrison BW, Moorman JR, Kowdley GC, Kobayashi YM, Jones LR, Leder P. Mat-8, a novel phospholemman-like protein expressed in human breast tumors, induces a chloride conductance in Xenopus oocytes. *J Biol Chem.* 1995; 270: 2176–2182.

5. Minor NT, Sha Q, Nichols CG, Mercer RW. The gamma subunit of the Na,K-ATPase induces cation channel activity. *Proc Natl Acad Sci USA.* 1998; 95: 6521–6525.

6. Moorman JR, Ackerman SJ, Kowdley GC, Griffin M, Mounsey JP, Chen Z, Cala SE, O'Brian JJ, Szabo G, Jones LR. Unitary onion currents through phospholemman channel molecules. *Nature.* 1995; 377: 737–740.

7. Wang X, Gao G, Guo K, Yarotskyy V, Huang C, Elmslie KS, Peterson BZ. Phospholemman modulates the gating of cardiac L-type calcium channels. *Biophys J.* 2010; 98: 1149–1159.

8. Jia LG, Donnet C, Bogaev RC, Blatt RJ, McKinney CE, Day KH, Berr SS, Jones LR, Moorman JR, Sweadner KJ, et al. Hypertrophy, increased ejection fraction, and reduced Na-K-ATPase activity in phospholemman-deficient mice. *Am J Physiol Heart Circ Physiol.* 2005; 288: H1982–H1988.

9. Zhang XQ, Moorman JR, Ahlers BA, Carl LL, Lake DE, Song J, Mounsey JP, Tucker AL, Chan YM, Rothblum LI, et al. Phospholemman overexpression inhibits Na^+-K^+-ATPase in adult rat cardiac myocytes: relevance to decreased Na^+ pump activity in post-infarction myocytes. *J Appl Physiol.* 2006; 100: 212–220.

10. Zhang XQ, Qureshi A, Song J, Carl LL, Tian Q, Stahl RC, Carey DJ, Rothblum LI, Cheung JY. Phospholemman modulates Na^+/Ca^{2+} exchange in adult rat cardiac myocytes. *Am J Physiol Heart Circ Physiol.* 2003; 284: H225–H233.

11. Song J, Zhang XQ, Carl LL, Qureshi A, Rothblum LI, Cheung JY. Overexpression of phospholemman alter contractility and $[Ca^{2+}]_i$ transients in adult rat myocytes. *Am J Physiol Heart Circ Physiol.* 2002; 283: H576–H583.

12. Mirza MA, Zhang XQ, Ahlers BA, Qureshi A, Carl LL, Song J, Tucker AL, Mounsey JP, Moorman JR, Rothblum LI, et al. Effects of phospholemman downregulation on contractility and $[Ca^{2+}]_i$ transients in adult rat cardiac myocytes. *Am J Physiol Heart Circ Physiol.* 2004; 286: H1322–H1330.

13. Song J, Zhang XQ, Ahlers BA, Carl LL, Wang J, Rothblum LI, Stahl RC, Mounsey JP, Tucker AL, Moorman JR, et al. Serine 68 of phospholemman is critical in modulation of contractility, $[Ca^{2+}]_i$ transients, and Na^+/Ca^{2+} exchange in adult rat cardiac myocytes. *Am J Physiol Heart Circ Physiol.* 2005; 288: H2342–H2354.

14. Lu KP, Kemp BE, Means AR. Identification of substrate specificity determinants for the cell cycle-regulated NIMA protein kinase. *J Biol Chem.* 1994; 269: 6603–6607.

15. Waalas SI, Czernik AJ, Olstad OK, Sletten K, Walaas O. Protein kinase C and cyclic AMP-dependent protein kinase phosphorylate phospholemman, an insulin and adrenaline-regulated membrane phosphoprotein, at specific sites in the carboxy terminal domain. *Biochem J.* 1994; 304: 635–640.

16. Mounsey JP, John III JE, Helmke SM, Bush EW, Gilbert J, Roses AD, Perryman MB, Jones LR, Moorman JR. Phospholemman is a substrate for myotonic dystrophy protein kinase. *J Biol Chem.* 2000; 275: 23362–23367.

17. Presti CF, Jones LR, Lindemann JP. Isoproterenol-induced phosphorylation of a 15-kilodalton sarcolemmal protein in intact myocardium. *J Biol Chem.* 1985; 260: 3860–3867.

18. Despa S, Bossuyt J, Han F, Ginsburg KS, Jia LG, Kutchai H, Tucker AL, Bers DM. Phospholemman-phosphorylation mediates the β-adrenergic effects on Na/K pump function in cardiac myocytes. *Circ Res.* 2005; 97: 252–259.

19. Han F, Bossuyt J, Despa S, Tucker AL, Bers DM. Phospholemman phosphorylation mediates the protein kinase C-dependent effects on Na^+/K^+ pump function in cardiac myocytes. *Circ Res.* 2006; 99: 1376–1383.

20. Wang J, Gao E, Song J, Zhang XQ, Li J, Koch WJ, Tucker AL, Philipson KD, Chan TO, Feldman AM, et al. Phospholemman and β-adrenergic stimulation in the heart. *Am J Physiol Heart Circ Physiol.* 2010; 298: H807–H815.

21. Silverman BD, Fuller W, Eaton P, Deng J, Moorman JR, Cheung JY, James AF, Shattock MJ. Serine68 phosphorylation of phospholemman: acute isoform-specific activation of cardiac Na/K ATPase. *Cardiovasc Res.* 2005; 65: 93–103.

22. Zhang XQ, Ahlers BA, Tucker AL, Song J, Wang J, Moorman JR, Mounsey JP, Carl LL, Rothblum LI, Cheung JY. Phospholemman inhibition of the cardiac Na^+/Ca^{2+} exchanger. Role of phosphorylation. *J Biol Chem.* 2006; 281: 7784–7792.

23. Despa S, Tucker AL, Bers DM. PLM-mediated activation of Na/K-ATPase limits $[Na]_i$ and inotropic state during β-adrenergic stimulation in mouse ventricular myocytes. *Circulation.* 2008; 117: 1849–1855.

24. Song J, Zhang XQ, Wang J, Cheskis E, Chan TO, Feldman AM, Tucker AL, Cheung JY. Regulation of cardiac myocyte contractility by phospholemman: Na^+/Ca^{2+} exchange vs. Na^+-K^+-ATPase. *Am J Physiol Heart Circ Physiol.* 2008; 295: H1615–H1625.

25. Wang J, Gao E, Rabinowitz J, Song J, Zhang XQ, Koch WJ, Tucker AL, Chan TO, Feldman AM, Cheung JY. Regulation of in vivo cardiac contractility by phospholemman: role of Na^+/Ca^{2+} exchange. *Am J Physiol Heart Circ Physiol.* 2011; 300: H859–H868.

26. Sehl PD, Tai JT, Hillan KJ, Brown LA, Goddard A, Yang R, Jin H, Lowe DG. Application of cDNA microarrays in determining molecular phenotype in cardiac growth, development, and response to injury. *Circulation.* 2000; 101: 1990–1999.

27. Tucker AL, Song J, Zhang XQ, Wang J, Ahlers BA, Carl LL, Mounsey JP, Moorman JR, Rothblum LI, Cheung JY. Altered contractility and $[Ca^{2+}]_i$ homeostasis in phospholemman-deficient murine myocytes: role of Na^+/Ca^{2+} exchange. *Am J Physiol Heart Circ Physiol.* 2006; 291: H2199–H2209.

28. Zhou YY, Wang SQ, Zhu WZ, Chruscinski A, Kobilka BK, Ziman B, Wang S, Lakatta EG, Cheng H, Xiao RP. Culture and adenoviral infection of adult mouse cardiac myocytes: methods for cellular genetic physiology. *Am J Physiol Heart Circ Physiol.* 2000; 279: H429–H436.

29. van den Borne SW, van de Schans VA, Strzelecka AE, Vervoort-Peters HT, Lijnen PM, Cleutjens JP, Smits JF, Daemen MJ, Janssen BJ, Blankesteijn WM. Mouse strain determines the outcome of wound healing after myocardial infarction. *Cardiovasc Res.* 2009; 84: 273–282.

30. Zhang XQ, Musch TI, Zelis R, Cheung JY. Effects of impaired Ca^{2+} homeostasis on contraction in postinfarction myocytes. *J Appl Physiol.* 1999; 86: 943–950.

31. Zhang XQ, Tillotson DL, Moore RL, Zelis R, Cheung JY. Na^+/Ca^{2+} exchange currents and SR Ca^{2+} contents in postinfarction myocytes. *Am J Physiol Cell Physiol.* 1996; 271: C1800–C1807.

32. Zhang XQ, Ng YC, Moore RL, Musch TI, Cheung JY. In situ SR function in postinfarction myocytes. *J Appl Physiol.* 1999; 87: 2143–2150.

33. Dixon IMC, Hata T, Dhalla NS. Sarcolemmal calcium transport in congestive heart failure due to myocardial infarction in rats. *Am J Physiol Heart Circ Physiol.* 1992; 262: H1387–H1394.

34. Zhang XQ, Song J, Qureshi A, Rothblum LI, Carl LL, Tian Q, Cheung JY. Rescue of contractile abnormalities by Na^+/Ca^{2+} exchanger overexpression in postinfarction rat myocytes. *J Appl Physiol.* 2002; 93: 1925–1931.

35. Cheung JY, Zhang XQ, Song J, Gao E, Rabinowitz JE, Chan TO, Wang J. Phospholemman: a novel cardiac stress protein. *Clin Transl Sci.* 2010; 3: 189–196.

36. Zhang XQ, Ng YC, Musch TI, Moore RL, Zelis R, Cheung JY. Sprint training attenuates myocyte hypertrophy and improves Ca^{2+} homeostasis in postinfarction myocytes. *J Appl Physiol.* 1998; 84: 544–552.

37. Quinn FR, Currie S, Duncan AM, Miller S, Sayeed R, Cobbe SM, Smith GL. Myocardial infarction causes increased expression but decreased activity of the myocardial Na^+–Ca^{2+} exchanger in the rabbit. *J Physiol (Lond).* 2003; 553: 229–242.

38. Bossuyt J, Ai X, Moorman JR, Pogwizd SM, Bers DM. Expression and phosphorylation of the Na-pump regulatory subunit phospholemman in heart failure. *Circ Res.* 2005; 97: 558–565.

39. Zhang XQ, Moore RL, Tillotson DL, Cheung JY. Calcium currents in postinfarction rat cardiac myocytes. *Am J Physiol Cell Physiol.* 1995; 269: C1464–C1473.

40. Marx SO, Reiken S, Hisamatsu Y, Jayaraman T, Burkhoff D, Rosemblit N, Marks AR. PKA phosphorylation dissociates FKBP12.6 from the calcium release channel (ryanodine receptor): defective regulation in failing hearts. *Cell.* 2000; 101: 365–376.

41. Jiang MT, Lokuta AJ, Farrell EF, Wolff MR, Haworth RA, Valdivia HH. Abnormal Ca^{2+} release, but normal ryanodine receptors, in canine and human heart failure. *Circ Res.* 2002; 91: 1015–1022.

42. Tadros GM, Zhang XQ, Song J, Carl LL, Rothblum LI, Tian Q, Dunn J, Lytton J, Cheung JY. Effects of Na^+/Ca^{2+} exchanger downregulation on contractility and $[Ca^{2+}]_i$ transients in adult rat myocytes. *Am J Physiol Heart Circ Physiol.* 2002; 283: H1616–H1626.

43. Zhang XQ, Song J, Rothblum LI, Lun M, Wang X, Ding F, Dunn J, Lytton J, McDermott PJ, Cheung JY. Overexpression of Na^+/Ca^{2+} exchanger alters contractility and SR Ca^{2+} content in adult rat myocytes. *Am J Physiol Heart Circ Physiol.* 2001; 281: H2079–H2088.

44. Mattiello JA, Margulies KB, Jeevanandam V, Houser SR. Contribution of reverse-mode sodium-calcium exchange to contractions in failing human left ventricular myocytes. *Cardiovasc Res.* 1998; 37: 424–431.

45. Gaughan JP, Furukawa S, Jeevanadam V, Hefner CA, Kubo H, Margulies KB, McGowan BS, Mattiello JA, Dipla K, Piacentino III V, et al. Sodium/calcium exchange contributes to contraction and relaxation in failed human ventricular myocytes. *Am J Physiol Heart Circ Physiol.* 1999; 277: H714–H724.

46. Dipla K, Mattiello JA, Margulies KB, Jeevanandam V, Houser SR. Sarcoplasmic reticulum and the Na^+/Ca^{2+} exchanger both contribute to the Ca^{2+} transient of failing human ventricular myocytes. *Circ Res.* 1999; 84: 435–444.

47. Hampton TG, Wang JF, DeAngelis J, Amende I, Philipson KD, Morgan JP. Enhanced gene expression of Na^+/Ca^{2+} exchanger attenuates ischemic and hypoxic contractile dysfunction. *Am J Physiol Heart Circ Physiol.* 2000; 279: H2846–H2854.

48. Min J-Y, Sullivan MF, Yan X, Feng X, Chu V, Wang J-F, Amende I, Morgan JP, Philipson KD, Hampton TG. Overexpression of Na^+/Ca^{2+} exchanger gene attenuates postinfarction myocardial dysfunction. *Am J Physiol Heart Circ Physiol.* 2002; 283: H2466–H2471.

49. Zhang XQ, Zhang LQ, Palmer BM, Ng YC, Musch TI, Moore RL, Cheung JY. Sprint training shortens prolonged action potential duration in postinfarction rat myocyte: mechanisms. *J Appl Physiol.* 2001; 90: 1720–1728.

50. Nuss HB, Houser SR. Sodium-calcium exchange-mediated contractions in feline ventricular myocytes. *Am J Physiol Heart Circ Physiol.* 1992; 263: H1161–H1169.

51. Pogwizd SM, Schlotthauer K, Li L, Yuan W, Bers DM. Arrhythmogenesis and contractile dysfunction in heart failure: roles of sodium-calcium exchange, inward rectifier potassium current, and residual β-adrenergic responsiveness. *Circ Res.* 2001; 88: 1159–1167.

52. Song J, Zhang XQ, Wang J, Carl LL, Ahlers BA, Rothblum LI, Cheung JY. Sprint training improves contractility in postinfarction rat myocytes: role of Na^+/Ca^{2+} exchange. *J Appl Physiol.* 2004; 97: 484–490.

53. Wasserstrom JA, Holt E, Sjaastad I, Lunde PK, Odegaard A, Sejersted OM. Altered E-C coupling in rat ventricular myocytes from failing hearts 6 wk after MI. *Am J Physiol Heart Circ Physiol.* 2000; 279: H798–H807.

54. Litwin S, Bridge JH. Enhanced Na^+-Ca^{2+} exchange in the infarcted heart. Implications for excitation-contraction coupling. *Circ Res.* 1997; 81: 1083–1093.

55. Sipido KR, Volders PGA, Vos MA, Verdonck F. Altered Na/Ca exchange activity in cardiac hypertrophy and heart failure: a new target for therapy? *Cardiovasc Res.* 2002; 53: 782–805.

56. Bell JR, Kennington E, Fuller W, Dighe K, Donoghue P, Clark JE, Jia LG, Tucker AL, Moorman JR, Marber MS, et al. Characterisation of the phospholemman knockout mouse heart: depressed left ventricular function with increased Na/K ATPase activity. *Am J Physiol.* 2008; 294: H613–H621.